This paper uses Mayr-Cassie-Kizilcay models

Model-Based General Arcing Fault Detection in Medium-Voltage Distribution Lines

Wenhai Zhang, Yindi Jing, *Member, IEEE*, and Xianyong Xiao, *Member, IEEE*

***Abstract*—Arcing fault is a special fault in medium-voltage distribution lines which can potentially cause shock hazard, apparatuses failure, and wild fire. Due to its short duration or low fault current, the detection of an arcing fault in distribution lines is highly challenging. In this paper, a model-based general detection method to separate an arcing fault from common nonarcing disturbances is proposed. First, an arcing fault model and a nonarcing disturbance model relating the disturbance characteristics, the load parameters, and the substation voltage and current waveforms are derived. For the accuracy of the models, the voltage drop on the distribution line is taken into consideration. Then, the procedure of arcing fault detection is introduced, including disturbance current calculation, parameters estimation, mean-square-error calculation, and decision making. An arcing fault is claimed when the measured voltage and current signals match the arcing fault model better than the nonarcing disturbance model. The method is tested on a modified standard test system using PSCAD/EMTDC considering different fault locations and scenarios. Simulation results show that the proposed detection method has high accuracy and is robust to fault distance, fault resistance, load current, and sampling rate. Laboratory experiments are also conducted to further validate the proposed method.**

***Index Terms*—Arcing fault, binary hypothesis test, high impedance fault, incipient fault, medium-voltage (MV) distribution system, model based.**

I. Introduction

ARC is a continuous luminous discharge of electricity across an insulating medium which is changed into a conducting medium. It can produce a large amount of heat in a short time and be dangerous to the safety of human beings and power system apparatuses. In medium voltage (MV) distribution lines, arcing fault may cause cable explosion when it occurs in underground cable [1] and may cause wildfire hazards [2] when it occurs in overhead line, e.g., when the down conductor is in contact with a high impedance surface such as asphalt road, macadam, grass or sand [3]. So accurate arcing fault detection is very important for the safety of people and distribution systems.

Arc is closely connected with several types of faults in MV distribution lines. It is widely accepted that the incipient fault contains arc [4], especially the incipient fault in underground cable [5]. The transient fault in overhead line is also commonly accompanied by arc [6]. The current of these arcing faults can reach several kilo-amperes, thus they are referred to as high current arcing fault. But the faults may only last from half-cycle to several cycles due to the self-clearing feature [7]. Also, the high impedance fault (HIF) always occurs with arc, where the fault current is usually just several tens of amperes [3]. Such fault is referred to as low current arcing fault [8].

Due to these close connections, the development of arcing fault detection schemes can help the detection of incipient fault, transient fault and HIF; hence is crucial in enhancing the reliability of MV systems. For example, arcing fault detection is an important way to recognize transient fault from permanent fault for enhancing the success rate of autoreclosure [6]. Most current MV distribution systems rely on the inverse-time overcurrent relay for its protection. The larger the current magnitude above the pickup value of the device, the sooner the device will time out and trigger the interruption of the current [9]. But this overcurrent protection is incapable in detecting arcing faults, characterized by either short duration or low magnitude [7].

In past decades, there have been a large number of studies on arcing fault detection. Some recent work on high current arcing fault are [6], [10], [11], where the authors took advantage of the feature that the arc voltage mimics a distorted rectangular waveform. In [6], the arcing fault voltage was modeled as an ideal rectangular waveform and the detection was based on the value of the expected rectangular amplitude estimated from the substation voltage information. In [10], the rectangular feature was recognized as a harmonic source and the fault phase total harmonic distortion was used for detection. [11] also followed the frequency-domain harmonic analysis. Detailed frequency domain fault equations were built to estimate fault resistance for arcing fault detection.

For low current arcing fault, many detection schemes have been proposed (e.g., [12]–[15]) and an extensive review of the detection methods were summarized in [3]. Commonly, the fault current distortion feature is utilized for the detection [12]–[14]. In [12], it was proposed to use the even order harmonic current variation for high impedance fault detection. In [13], a time-frequency analysis was used and the detection was based on the current waveform energy and normalized joint time-frequency

Manuscript received August 18, 2015; revised November 24, 2015; accepted January 09, 2016. Date of publication January 25, 2016; date of current version September 21, 2016. This work was supported in part by the China Scholarship Council under Grant 201406240005 and in part by the Miaozi Project in Science and Technology Innovation Program of Sichuan Province under Grant 2015MZGC001. Paper no. TPWRD-01107-2015.

W. Zhang and X. Xiao are with the College of Electrical Engineering and Information Technology, Sichuan University, Chengdu 610065, China (e-mail: zhangwh1989@163.com; xiaoxianyong@163.com).

Y. Jing is with the Department of Electrical and Computer Engineering, University of Alberta, Edmonton, AB T6G 1H9 Canada (e-mail: yindi@ualberta.ca).

Color versions of one or more of the figures in this paper are available online at http://ieeexplore.ieee.org.

Digital Object Identifier 10.1109/TPWRD.2016.2518738

moments extracted from current signals. In [14], wavelet transform was applied to extract fault feature and artificial neural network structure and learning algorithm were used for detection. The scheme proposed in [15] is based on voltage signals, where a transformation based on set theory and integral geometry was used for the voltage analysis.

But all existing work are on either high current or low current arcing fault. There is no method that can detect both types in MV systems simultaneously. In reality, the division between high current and low current arcing faults is vague, and sometimes, it is unclear how to choose the proper method. So, a general detection method that can treat a wide range of arcing faults is very useful and highly desirable.

In response to the challenge, this paper proposes an (arc) model-based general arcing fault detection method. Different from the traditional methods, it formulates the problem as the estimation of parameters for an arc model. In addition, a binary hypothesis test is applied to discriminate an arcing fault from a non-arcing disturbance (such as load switching, motor starting, and constant impedance faults). The proposed method has been tested on a modified IEEE 13-node test feeder simulated using PSCAD/EMTDC. Simulation results show that the method has very high accuracy in detecting an arcing fault from the voltage and current waveforms measured at the substation. Laboratory tests on underground cable are also conducted. The results show that the method can detect arcing fault accurately and causes no false detection.

The remainder of this paper is organized as follows. Section II presents the detection problem, the system models and the binary hypothesis test formulation. In Section III, the model-based detection solution is provided, including the parameter estimation method, the detection rule and a summary of the detection procedure. Simulation results are presented in Section IV. Section V shows laboratory test results on underground cable. Finally, conclusions are drawn in Section VI.

II. Hypothesis Testing Model for Arcing Fault Detection

The focus of this work is to detect whether a disturbance in an MV distribution system is an arcing fault from the voltage and current waveforms observed at the substation. It is assumed that a disturbance (e.g., arcing fault, constant impedance fault, disturbance caused by load switching or motor starting) has already been acknowledged and the time stamp of the fault is known. Our goal is to discriminate arcing faults from other disturbances such as constant impedance fault, load switching, and motor starting from the signals in question. By following detection theory [16], the problem can naturally be recognized as a binary hypothesis test. The two hypotheses denoted as H_0 and H_1 are as follows:

$$H_0 : \text{An arcing fault},$$
$$H_1 : \text{A non}-\text{arcing disturbance}.$$

In what follows, we first propose a model for the distribution system with a disturbance branch, then introduce arcing fault model and non-arcing disturbance model for the branch in question, and finally present the mathematical formulation for the binary hypothesis testing.

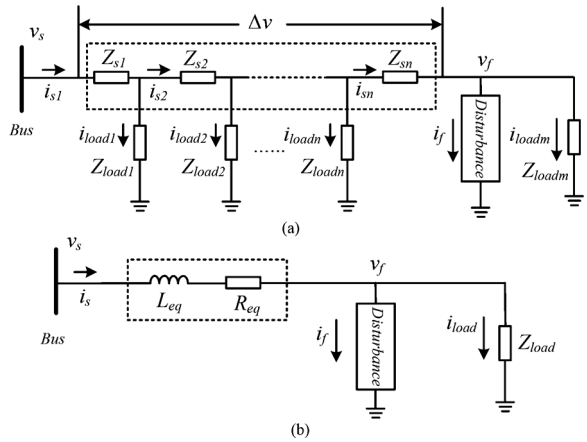

Fig. 1. Models for an MV distribution system with a disturbance branch. (a) The physical model considering load branches and line section impedance. (b) The simplified model.

A. Proposed Model for Distribution System With Disturbance

An MV distribution system with a disturbance branch can be represented by Fig. 1(a), where $v_s(t)$ and $i_s(t)$ are the voltage and current signals measured at the substation. Without loss of generality, assume that there are n load branches before the disturbance branch. The symbols $i_{s_1}(t), \ldots, i_{s_n}(t)$ denote the currents in the line sections before the load branches and $Z_{s_1}, \ldots, Z_{s_n}$ denote the line section impedances, where each is composed of a resistance component R_{s_n} and an inductance component L_{s_n}. The voltage and current of the disturbance branch is denoted by $v_f(t)$ and $i_f(t)$, respectively. Notice that all loads after the fault branch can be equivalently represented as one load branch. We use $i_{load}(t)$ and Z_{load} to denote the total load current and load impedance of such branch. The time symbol t is omitted in the figure for the voltage and current signals for simplicity.

While only the substation voltage and current can be measured, we are interested in the disturbance branch and need to detect whether the disturbance is an arcing fault. Since the location of the disturbance is unknown, neither the number of the load branches before the disturbance nor their parameters are known. Thus, in what follows, we derive an equivalent model for the distribution system that allows more direct connection between the substation power signals and the disturbance branch power signals. The voltage drop $\Delta v(t)$ between the substation and the disturbance branch caused by line impedance is considered for the precision of our model and analysis. The line impedance cannot be ignored because it is very large compared with arc resistance.

From Fig. 1(a), we have

$$v_s(t) = \Delta v(t) + v_f(t)$$
and
$$\Delta v(t) = \sum_{k=1}^{n} i_{s_k}(t) \cdot R_{s_k} + \sum_{k=1}^{n} L_{s_k} \cdot \frac{di_{s_k}(t)}{dt}. \quad (1)$$

We assume that all currents flows between the substation and disturbance branch are approximately proportional to the substation current, i.e.,

$$i_{s_k}(t) = \lambda_k \cdot i_s(t), \quad \text{for } k = 1, \ldots, n,$$

where $\lambda_1, \lambda_2, \ldots, \lambda_n$ are constant. This assumption is generally valid when a feeder has a large number of distributed loads. From (1), we obtain

$$\Delta v(t) = \left(\sum_{k=1}^{n} \lambda_k R_{s_k}\right) \cdot i_s(t) + \left(\sum_{k=1}^{n} \lambda_k L_{s_k}\right) \cdot \frac{di_s(t)}{dt}. \quad (2)$$

Define

$$R_{eq} = \sum_{k=1}^{n} \lambda_k R_{s_k}, \quad L_{eq} = \sum_{k=1}^{n} \lambda_k L_{s_k}.$$

(2) leads to

$$\Delta v(t) = R_{eq} \cdot i_s(t) + L_{eq} \cdot \frac{di_s(t)}{dt}. \quad (3)$$

R_{eq} and L_{eq} are the equivalent resistance and inductance between the substation and the disturbance branch. With these derivations, we obtain a simplified model for the distribution system, which is shown in Fig. 1(b).

The following connection between the voltage measured at the substation and the voltage of the disturbance branch is thus derived:

$$v_s(t) = R_{eq} \cdot i_s(t) + L_{eq} \cdot \frac{di_s(t)}{dt} + v_f(t) + n(t), \quad (4)$$

where $n(t)$ is the noise component. It can represent measurement noise, modeling error and any other uncertainties and disturbances experienced by the distribution system.

In the next two subsections, we introduce models for the disturbance branch of the distribution system for the two cases: the branch has an arcing fault and the branch has a non-arcing disturbance.

B. Arcing Fault Model

With generality, in a distribution system, a branch with an arcing fault can be modeled as an arc in series with a constant resistance R_0 [17], as shown in Fig. 2, where $R_{arc}(t)$ is the time-varying arc resistance. Let $g_{arc}(t) = 1/R_{arc}(t)$ be the arc conductance, which is also time-varying. Thus,

$$v_f(t) = i_f(t) \cdot R_0 + \frac{i_f(t)}{g_{arc}(t)}, \quad (5)$$

An arc model to describe $g_{arc}(t)$ is needed for the modeling of the detection problem.

The research on arc model have been conducted for several decades and many arc models have been proposed for different motivations, e.g., circuit-breaker arc analysis [18], arc energy calculation [19] and arcing fault analysis [17], [20]–[23]. In this paper, we use the Kizilcay's model which is a dynamic arc model

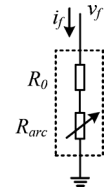

Fig. 2. The general arcing fault model.

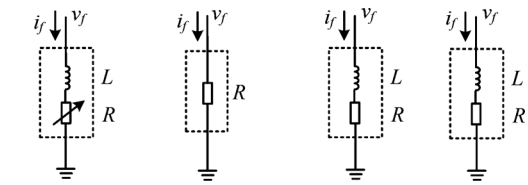

Fig. 3. Common non-arcing disturbance models and the general R-L model.

derived from the viewpoint of control theory based on the energy balance in the arc column [20]. The model has been tested and proved to be accurate [21]. It has also been utilized in many arcing fault analysis [17], [22], [23]. The arc model that connects $g_{arc}(t)$ and the current of the arc branch $i_f(t)$ is as follows:

$$\frac{dg_{arc}(t)}{dt} = \frac{1}{\tau}\left(\frac{|i_f(t)|}{u_0 + r_0|i_f(t)|} - g_{arc}(t)\right), \quad (6)$$

where u_0 is the characteristic arc voltage, r_0 is the characteristic arc resistance, and τ is the arc time constant.

C. Non-Arcing Disturbance Model

In this subsection, we present a model for the disturbance branch when the disturbance is not an arcing fault. Typical non-arcing disturbance includes constant impedance fault, motor starting and load switching. The models of these disturbances are shown in Fig. 3. It is noted that although the motor starting model is a dynamic model, it can actually be recognized as static model in short time (within two cycles). For load switching, even though rigorously speaking there are non-linear loads, but since the numbers of loads and load branches in a typical distribution system are very large, the effect of non-linear loads is diluted and made negligible by other loads. Thus, statistically speaking, it can be well modeled by an R-L model. So non-arcing disturbances can be generally recognized as a series of a constant resistance R and a constant inductance L as shown in Fig. 3. Thus for the distribution system with a non-arcing disturbance, we have

$$v_f(t) = i_f(t) \cdot R + L \cdot \frac{di_f(t)}{dt}. \quad (7)$$

D. Hypothesis Testing Formulation for Arcing Fault Detection

With the derivations and discussions in Sections II.A to Section II.C, we can obtain models for the distribution system under the two hypotheses (H_0: an arcing fault and H_1: a non-arcing disturbance) as shown in Fig. 4(a) and (b), respectively.

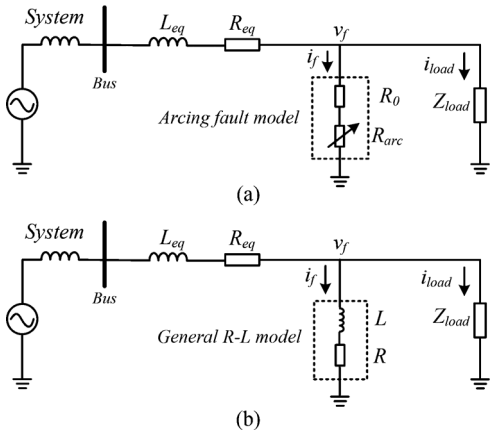

Fig. 4. General arcing fault model and non-arcing disturbance model in distribution system. (a) The general arcing fault. (b) The non-arcing disturbance.

The binary hypothesis testing problem to detect an arcing fault in the distribution system can be formulated as follows:

$$H_0: \begin{cases} v_s(t) = R_{eq}\cdot i_s(t) + L_{eq}\cdot \frac{di_s(t)}{dt} \\ \qquad\qquad +i_f(t)\cdot R_0 + \frac{i_f(t)}{g_{arc}(t)} + n(t), \\ \frac{dg_{arc}(t)}{dt} = \frac{1}{\tau}\left(\frac{|i_f(t)|}{u_0 + r_0|i_f(t)|} - g_{arc}(t)\right). \end{cases} \tag{8}$$

$$H_1: v_s(t) = R_{eq}\cdot i_s(t) + L_{eq}\cdot \frac{di_s(t)}{dt} + R\cdot i_f(t) + L\cdot \frac{di_f(t)}{dt} + n(t). \tag{9}$$

Equation (8) is obtained by using (5) in (4) and (9) is obtained by using (7) in (4). The problem is to test which hypothesis is true given the voltage signal $v_s(t)$ and current signal $i_s(t)$ measured at the substation.

III. Parameter Estimation and Arcing Fault Detection

In this section, the procedure for arcing fault detection using the voltage and current signals measured at the substation are introduced in details, including disturbance current estimation, parameters estimation, voltage mean-square-error (MSE) calculation and decision making. In addition, we discuss possible issues in practical implementation. In real distribution systems, the measured voltage and current signals are discrete samples. Thus, in what follows we use $v_s(n)$ and $i_s(n)$ for $n = 1, 2, \ldots$ to denote the substation voltage and current values at time $n\Delta t$, where Δt is the sampling interval. Similar notation are used for other signals. The current differential $di_s(n)/dt$ can be calculated as:

$$\frac{di_s(n)}{dt} = \frac{i_s(n) - i_s(n-1)}{\Delta t}. \tag{10}$$

A. Calculation of the Disturbance Current i_f

To solve the detection problem, the disturbance current $i_f(n)$ needs to be calculated first. This can be done using feeder voltage $v_s(n)$ and feeder current $i_s(n)$ based on Fig. 4. We assume that the load is a constant impedance Z_{load} (including the load resistance R_{load} and inductance L_{load}) during the disturbance and shortly before the disturbance. Also, since the line impedance R_{eq} and L_{eq} are considerably smaller compared with R_{load} and L_{load}, in load impedance estimation and $i_{load}(n)$ calculation, the distribution line impedance is ignored. This approximation largely simplifies the parameter estimation and arcing fault detection processes. It is also commonly used in the literature [24]. It is noted that in the model simplification in Section II.A, the line impedance cannot be ignored as the line impedance may be very large compared with fault resistance.

With these assumptions, R_{load} and L_{load} can be reliably estimated from pre-disturbance current and voltage based on Ohm's law [24]. Thus, they can be treated as known parameters. By considering the load branch in Fig. 4, we have

$$v_s(n) \approx i_{load}(n)\cdot R_{load} + L_{load}\cdot \frac{i_{load}(n) - i_{load}(n-1)}{\Delta t},$$

from which

$$i_{load}(n) \approx \frac{v_s(n)\cdot \Delta t + L_{load}\cdot i_{load}(n-1)}{R_{load}\cdot \Delta t + L_{load}}. \tag{11}$$

Thus the load branch current $i_{load}(n)$ can be obtained recursively. The disturbance branch current can consequently be calculated as

$$i_f(n) = i_s(n) - i_{load}(n). \tag{12}$$

Its differential $di_f(n)/dt$ can be calculated as

$$\frac{di_f(n)}{dt} = \frac{i_f(n) - i_f(n-1)}{\Delta t}. \tag{13}$$

B. Estimation of Disturbance Parameters

We can see from the models in (8) and (9) that for both hypotheses, there are unknown parameters. Thus it is a composite hypothesis testing problem. Other than the unknown parameters for the distribution line R_{eq} and L_{eq}, for the arcing-fault hypothesis, the arc parameters R_0, τ, u_0, r_0 are unknown; for the non-arcing disturbance hypothesis, the R-L model parameters R and L are unknown. We propose to use least-squares estimation for the unknown parameter values. In what follows, the parameter estimation for H_0 is explained first, followed by that for H_1.

For the arcing-fault hypothesis H_0, from the second equation in (8), we have

$$\frac{g_{arc}(n) - g_{arc}(n-1)}{\Delta t} = \frac{1}{\tau}\left(\frac{|i_f(n)|}{u_0 + r_0|i_f(n)|} - g_{arc}(n)\right).$$

Thus, the arc conductance can be calculated as follows:

$$\begin{aligned} g_{arc}(n) &= \frac{\Delta t\cdot |i_f(n)|}{(\tau + \Delta t)\cdot (u_0 + r_0|i_f(n)|)} + \frac{\tau\cdot g_{arc}(n-1)}{\tau + \Delta t} \\ &= \frac{\Delta t}{\tau + \Delta t}\sum_{j=2}^{n} \frac{|i_f(n)|}{u_0 + r_0|i_f(n)|}\left(\frac{\tau}{\tau + \Delta t}\right)^{n-j} \\ &\quad + \left(\frac{\tau}{\tau + \Delta t}\right)^{n-1} g_{arc}(1). \end{aligned} \tag{14}$$

By setting $g_{arc}(1) = i_f(1)/v_s(1)$, $g_{arc}(n)$ is represented by the arc parameters u_0, r_0, τ and the disturbance branch current $i_f(n)$.

Now we are ready to conduct the least-squares estimation for the unknown parameters for the arcing fault hypothesis: $\mathbf{x}_0 = (R_{eq}, L_{eq}, R_0, \tau, u_0, r_0)$. By using (14) in the first equation of (8), the substation voltage $v_s(n)$ is represented as a function of the unknown vector $\mathbf{x}_0$ and the known data $data(n) = (i_s(n), di_s(n)/dt, i_f(n), di_f(n)/dt)$. We call this function F_0. The least-squares estimation problem for H_0 is described as the following optimization problem:

$$\hat{\mathbf{x}}_0 = \arg\min_{\mathbf{x}} \sum_{n=1}^{N} \left[F_0(x, data(n)) - v_s(n)\right]^2, \qquad (15)$$

where N is the total number of sampling points and $\hat{\mathbf{x}}_0 = (\hat{R}_{eq,0}, \hat{L}_{eq,0}, \hat{R}_0, \hat{\tau}, \hat{u}_0, \hat{r}_0)$ denotes the parameter estimation results. The *lsqcurvefit* function in MATLAB is used for the least-squares curve fitting.

As to the non-arcing disturbance hypothesis H_1, the unknown parameters are $\mathbf{x}_1 = (R_{eq}, L_{eq}, R, L)$ with the same $data(n)$. From (9), the substation voltage $v_s(n)$ is readily represented as a function of the unknown vector $\mathbf{x}_1$ and the known data $data(n)$. We call this function F_1. Similarly, the least-squares parameter estimation problem for H_1 is described as the following:

$$\hat{\mathbf{x}}_1 = \arg\min_{\mathbf{x}} \sum_{n=1}^{N} \left[F_1(x, data(n)) - v_s(n)\right]^2, \qquad (16)$$

where $\hat{\mathbf{x}}_1 = (\hat{R}_{eq,1}, \hat{L}_{eq,1}, \hat{R}, \hat{L})$ denotes the estimation results. Again, the *lsqcurvefit* function in MATLAB is used for the least-squares curve fitting.

It is noteworthy that when the noise $n(t)$ is a zero-mean white Gaussian random process or in other words when the sample noises $n(n\Delta t)$ are independent and identically distributed Gaussian random variables with zero-mean, the least squares estimation is the same as the optimal minimum MSE estimation. For other noise distributions, the estimation can be suboptimal.

C. Arcing-Fault Detection Rule and Summary of the Proposed Scheme

In this subsection, we explain the detection rule for the binary hypothesis testing. Intuitively, the detection result should depend on how well the data match each hypothesis. Thus, the curve-fitting error or MSE is used for detection. Under H_0, given the parameter estimation $\hat{\mathbf{x}}_0$, we can calculate the estimated substation voltage from (8) as

$$\hat{v}_{s,0}(n) = \hat{R}_{eq,0} \cdot i_s(n) + \hat{L}_{eq,0} \cdot \frac{di_s(n)}{dt} + i_f(n) \cdot \hat{R}_0 + \frac{i_f(n)}{\hat{g}_{arc}(n)},$$

where $\hat{g}_{arc}(t)$ can be calculated according to (14). The curve fitting error under H_0 is thus

$$e_{\text{arc}} = \frac{1}{N - n_0 + 1} \sum_{n=n_0}^{N} \left[v_s(n) - \hat{v}_{s,0}(n)\right]^2 \qquad (17)$$

where n_0 is a constant. In this error calculation, the first $n_0 - 1$ data points are discarded. This is due to the recursive calculations of the disturbance current i_f explained in Section III.A and the arc conductance g_{arc} explained in Section III.B. The data points at the beginning may be affected by the choice of the initial conditions and induce extra error. In simulation and laboratory tests, we choose $n_0 = N/8$.

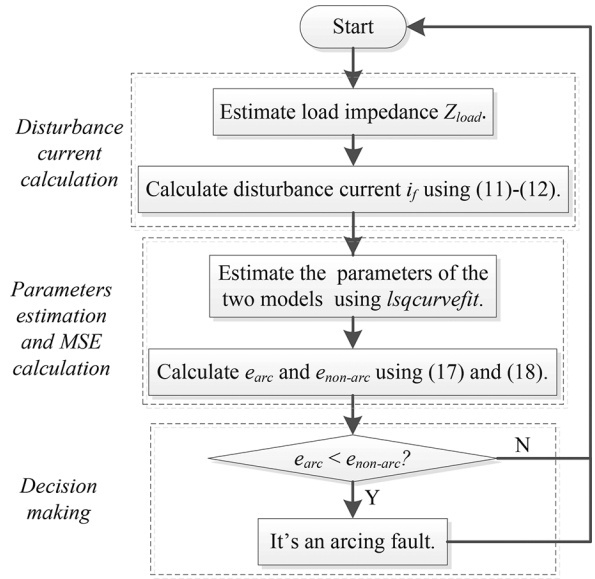

Fig. 5. The proposed procedure for arcing-fault detection.

Similarly, we can calculate the estimated substation voltage under H_1 from (8) as

$$\hat{v}_{s,1}(n) = \hat{R}_{eq,1} \cdot i_s(n) + \hat{L}_{eq,1} \cdot \frac{di_s(n)}{dt} + \hat{R} \cdot i_f(n) + \hat{L} \cdot \frac{di_f(n)}{dt}.$$

The fitting error under H_1 is thus

$$e_{\text{non-arc}} = \frac{1}{N - n_0 + 1} \sum_{n=n_0}^{N} \left[v_s(n) - \hat{v}_{s,1}(n)\right]^2. \qquad (18)$$

The detection rule is

$$H_0 : e_{\text{arc}} < e_{\text{non-arc}}$$
$$H_1 : e_{\text{arc}} \geq e_{\text{non-arc}}. \qquad (19)$$

In other words, if the error of fitting the arcing fault model is smaller, the detection result is H_0, an arcing fault; otherwise, the detection result is H_1, a non-arcing disturbance.

When the noise is a zero-mean white Gaussian random process, the detection rule is the same as the optimal likelihood ratio detection rule. The combined parameter estimation and detection method is the classic generalized likelihood ratio testing scheme for composite hypothesis testing problems.

The overall procedure of the proposed model-based arcing fault detection is shown in Fig. 5.

D. Discussions on Implementation

In this section, several issues for practical applications of the proposed method are discussed. Our method is based on feeder current and bus voltage waveforms. The measurement of the current and voltage signals can be done by current transformer (CT) and potential transformer (PT), which already exist in distribution systems. Digital fault recorders (DFRs) or intelligent electronic devices (IEDs) can be installed at the substation to capture waveform data with faults/disturbances and save the data.

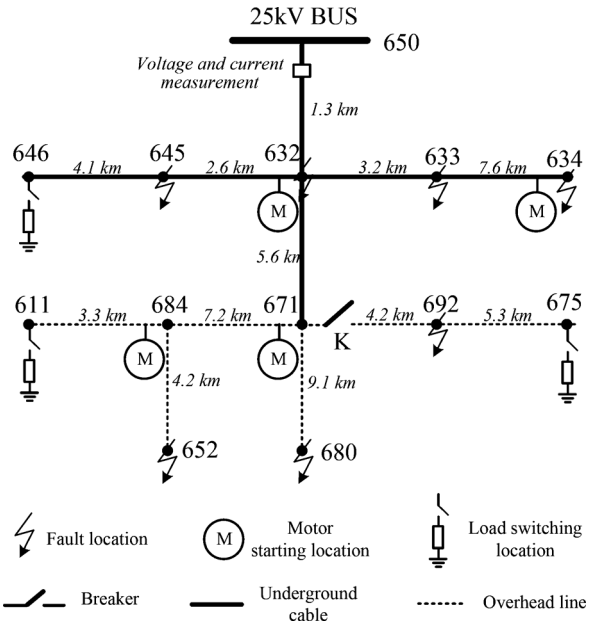

Fig. 6. Modified IEEE-13 node test feeder.

Current state-of-art devices can easily meet the measurement requirements of our proposed method. Based on our simulations, a sampling rate of 5 kHz is enough for the proposed detection method. This sampling rate is readily achieved by current DFRs and IEDs. Another issue is the CT frequency response, which affects the precision of the measurement. We can use protective CT which has good linearity even for measurements of large current signals. At 5 kHz sampling frequency, signals within 1 Hz–2.5 kHz are utilized for the detection. In fact, most traditional electromagnetic CTs and the more advanced electronic CTs have good frequency response in this frequency band [25]. Thus, the measurement is no more a problem especially with the widely use of electronic CTs with high measurement accuracy and frequency response.

IV. Simulation Results

In this section, simulation results are shown to validate the precision of the proposed model-based arcing fault detection method. A modified IEEE 13-node 25 kV test system considering both underground cable and overhead line is utilized, as shown in Fig. 6. While there are several possible disturbance locations, for any given time, only one disturbance happens in the system. In the simulations, different sampling rates, system structures and data lengths are considered.

The disturbances are produced by PSCAD/EMTDC. The multi-run function in PSCAD is used to simulate various kinds of disturbances with different parameters. The bus voltage and feeder current waveforms of these disturbances are saved. Then MATLAB is used to load the waveform data and conduct detection. For arcing faults, both high current arcing fault in underground cable and low current arcing fault in overhead line are considered. For non-arcing disturbances, we considered load switching, constant impedance fault and motor starting, which are difficult to be separated from arcing fault using traditional schemes. In what follows, we first elaborate on the parameters of arcing faults and non-arcing disturbances used in the simulation, then present the detection results of the proposed scheme.

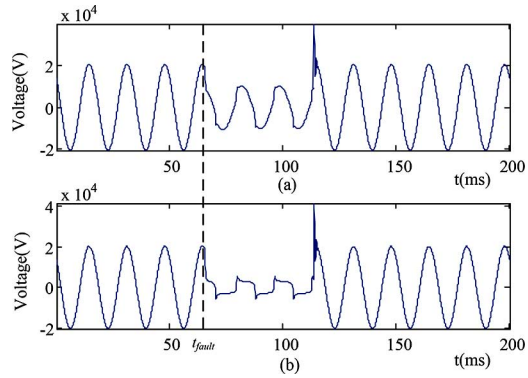

Fig. 7. Voltage waveforms of a high current arcing fault. (a) The bus voltage (v_s). (b) Fault point voltage (v_f).

A. Disturbance/Fault Types

Two types of arcing faults and three types of non-arcing disturbances are considered in the simulation. Their parameters and voltage/current characteristics are explained in this subsection.

1) High Current Arcing Fault: In MV distribution system, high current arcing fault always occurs in underground cable with low fault resistance. In our simulation, possible positions of arcing fault are 645, 632, 633 and 634 in Fig. 6. For this type of arcing fault, $R_0 = 0$. As to the other arc parameters, based on previous lab tests and field tests in underground cable [26]–[29], the ranges are as follows: τ : 0.05 $\sim$ 0.4 ms, u_0 : 300 $\sim$ 4000 V, r_0 : 0 $\sim$ 0.015 ohm. In the simulation, we generate a large number of high current arcing faults whose parameter values cover the whole ranges, The step sizes used for the 3 parameters are 0.15 ms, 200 V and 0.005 ohm.

The voltage waveforms of the substation voltage v_s and fault branch voltage v_f are shown in Fig. 7 for a high current arcing fault where the fault distance is 6 km and the arc parameters are $(\tau, u_0, r_0) = (0.0002, 2900, 0.001)$. The distortion on v_f is obvious and the signature square wave shape of an arcing fault can be clearly seen. However, the substation voltage v_s looks very close to sinusoidal and does not show obvious distortion compared with v_f.

2) Low Current Arcing Fault: The low current arcing fault always occurs in overhead line with the fault current between 15–100 A. In our simulations, possible fault locations are 652, 680 and 692 in Fig. 6. For this type of arcing fault, $R_0 \neq 0$. Its range is estimated based on phase voltage and fault current range, which is R_0 : 100 $\sim$ 900 ohm. Based on [26], the ranges of r_0, τ are chosen as τ : 0.05 $\sim$ 0.4 ms, and r_0 : 0 $\sim$ 0.015 ohm, respectively. As to u_0, there is no direct reference on its range. We use the current range for low current arcing fault and the relationship between arc voltage and current introduced in [30] to obtain the range for u_0, which is 1000 $\sim$ 6000 V. In our simulation, a large number of low current arcing faults are generated whose parameter values cover all the ranges. The step sizes for the 4 parameters (R_0, τ, u_0, r_0) are 200 ohm, 0.15 ms, 450 V, and 0.005 ohm, respectively.

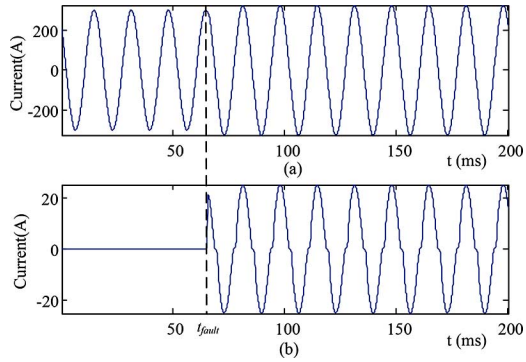

Fig. 8. Current waveforms of a low current arcing fault. (a) Feeder current measured at substation (i_s). (b) Fault current (i_f).

In Fig. 8, the waveforms of the substation current i_s and the fault current i_f are presented for a low current arcing fault where the fault distance is 8 km and the arc parameters are $(R_0, \tau, u_0, r_0) = (700, 0.0002, 2900, 0.004)$. It can be seen that the waveform of the simulated low current arcing fault is very similar to the field test ones in [31].

3) Non-Arcing Disturbances: Three types of non-arcing disturbance are used in the simulation: load switching, motor starting and constant impedance fault. These are the faults with similar features to arcing faults, thus it is very challenging to discriminate them from arcing faults. The possible locations are shown in Fig. 6. Wide ranges of parameter values of the non-arcing disturbances are used in the simulation. For constant impedance fault, the fault resistance is between 0.1 and 1500 ohm, for motor starting fault, the current ranges from 10 A to 100 A, for load switching fault, the load current is from 10 A to 80 A.

In Fig. 9, typical current waveforms for the non-arcing disturbances and arcing faults are compared. It can be seen that they have high similarity. The current waveform of constant impedance fault mimics that of large current arcing fault, and the current waveform of motor starting and load switching is close to that of low current arcing fault.

B. Detection Results

In this section, we present detection results of the proposed method when the breaker K in Fig. 6 is closed. Recall that for given substation voltage and current measurements, our method is to match the measurements with both the arcing-fault model (Hypothesis H_0) in (8) and the non-arcing disturbance model (Hypothesis H_1) in (9). The degrees of mismatch or model-fitting MSE are denoted as $e_{\rm arc}$ and $e_{\rm non-arc}$. The detection result is the one with a smaller MSE. Intuitively, larger difference between e_{arc} and $e_{non-arc}$ means higher detection robustness.

In Fig. 10(a), the MSEs ($e_{\rm arc}$ and $e_{\rm non-arc}$) for high current arcing faults with different u_0 are shown. The parameter u_0 is chosen since it is the most sensitive parameter of our proposed scheme. We can see that for all u_0 values, $e_{\rm arc} < e_{\rm non-arc}$ always. Thus our detection rule in (19) will always produce the correct detection result. The difference of the two MSEs gets larger when u_0 increases. Fig. 10(b) is for low current arcing faults with different R_0 values. We can see that for all R_0 values,

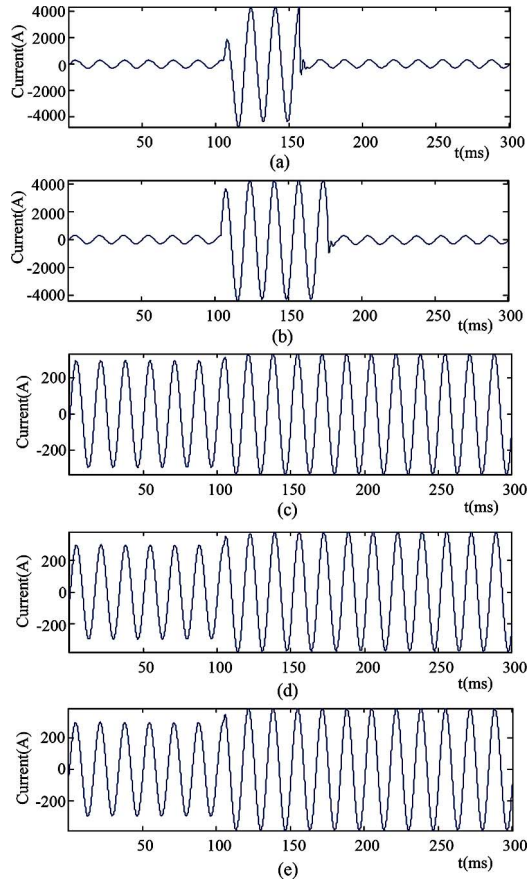

Fig. 9. Current waveforms of an arcing fault and non-arcing disturbances. (a) High current arcing fault in underground cable. (b) Constant impedance fault. (c) Low current arcing fault in overhead line. (d) Motor starting current. (e) Load switching current.

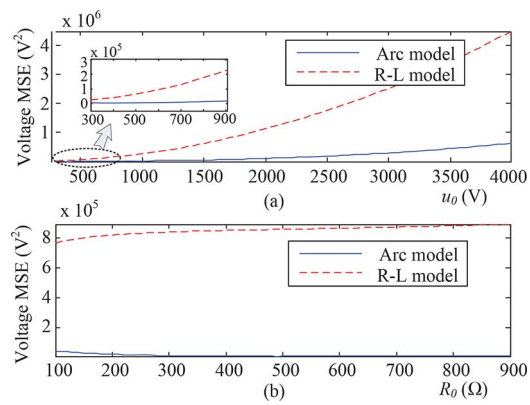

Fig. 10. MSE comparison for high current and low current arcing faults. (a) Voltage MSE comparison with different $u_0 (R_0 = 0, \tau = 0.0002, r_0 = 0.004)$. (b) Voltage MSE comparison with different $R_0 (\tau = 0.0002, u_0 = 2000, r_0 = 0.004)$.

$e_{\rm arc} < e_{\rm non-arc}$ always and there is a large gap between the two MSE curves.

Results on non-arcing disturbances are shown in Fig. 11 for different parameter values. We can see that for all three types of non-arcing disturbance, $e_{\rm arc} > e_{\rm non-arc}$ always, thus the proposed detection scheme always produces the correct detection

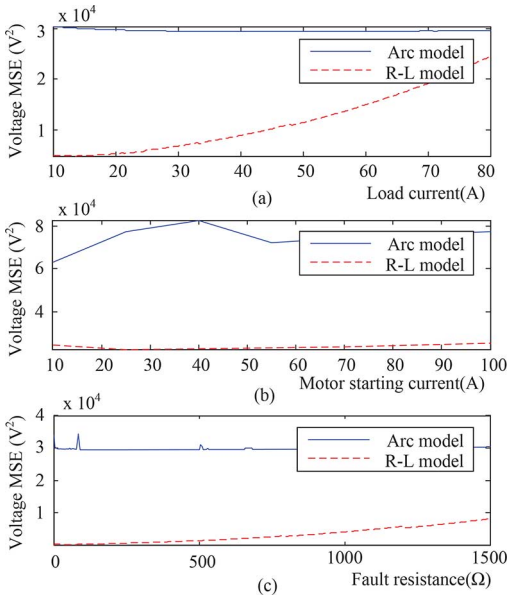

Fig. 11. MSE comparison for non-arcing disturbances. (a) Voltage MSE comparison with different load currents (load power factor = 0.9). (b) Voltage MSE comparison with different motor starting currents. (c) Voltage MSE comparison with different fault resistances.

TABLE I
DETECTION ACCURACY V.S. DATA LENGTH (SAMPLING RATE: 10 KHZ)

Disturbances	Case number	Detection rate (%)		
		0.5 cycle	1 cycle	2 cycles
High current arcing fault	960	98.44	98.85	99.06
Low current arcing fault	1485	100	100	100
Constant impedance fault	532	100	100	100
Load switching	435	100	100	100
Motor starting	32	100	100	100

result. The gap between the two MSE curves are significant, indicating high robustness of the proposed scheme.

C. Sensitivity Study

In this subsection, we present simulation results to show the sensitivity and robustness of the proposed scheme.

1) The Effect of Disturbance Duration: We first consider faults with different fault durations. The correct detection probability for different cases are shown in Table I where the sampling rate is 10 kHz (so there are 166 points per cycle for 60 Hz system). The data lengths used for detection are 0.5, 1 and 2 cycles. We can see that for all disturbance types except high current arcing fault, the proposed scheme achieve 100% detection accuracy even when the data length is as small as 0.5 cycle. For high current arcing fault, the detection accuracy is above 98% and increases as the data length increases. For non-arcing disturbances, there is no false detection as shown in Rows 3–5 of Table I.

2) The Effect of Sampling Rate: In order to verify the robustness of the method, we also conduct simulate at a lower sampling rate of 5 kHz. The results are shown in Table II. We can see that with the lower sampling rate, our scheme still achieves 100% detection precision for constant impedance fault, load switching and motor starting. For high and low current arcing faults, the detection probabilities are above 88% and 95%, respectively. As the data lengths grows, the accuracy increases.

TABLE II
DETECTION ACCURACY V.S. DATA LENGTH (SAMPLING RATE: 5 KHZ)

Disturbances	Case number	Detection rate (%)		
		0.5 cycle	1 cycle	2 cycles
High current arcing fault	960	88.74	92.49	92.49
Low current arcing fault	1485	95.42	96.09	96.9
Constant impedance fault	532	100	100	100
Load switching	435	100	100	100
Motor starting	32	100	100	100

TABLE III
DETECTION ACCURACY V.S. SNR

Disturbances	Case number	Detection rate (%)		
		80dB	70dB	60dB
High current arcing fault	960	98.85	98.74	98.64
Low current arcing fault	1485	100	100	99.66
Constant impedance fault	532	100	99.24	98.68
Load switching	435	100	99.54	98.85
Motor starting	32	100	100	96.88

TABLE IV
DETECTION ACCURACY V.S. DATA LENGTH WHEN BREAKER K IS OPEN

Disturbances	Case number	Detection rate (%)		
		0.5 cycle	1 cycle	2 cycles
High current arcing fault	960	98.74	99.17	99.37
Low current arcing fault	990	100	100	100
Constant impedance fault	456	100	100	100
Load switching	290	100	100	100
Motor starting	32	100	100	100

3) The Effect of Noise: To see the effect of measurement noise, we add white Gaussian noise to the current and voltage signals. The sampling rate is 10 kHz and data length is 1 cycle. The results are shown in Table III. Naturally, the detection precision decreases with the signal-noise-ratio (SNR). However it is larger than 98% even with when the SNR is 60 dB or higher. When the SNR is too low, filters can be applied for denoising.

4) The Effect of System Topology: In order to test the effect of system topology, we change system typology in our simulation by opening the breaker K in Fig. 6. The detection results are given in Table IV. Comparing with Table I, we can see that the detection accuracy is similar to those when breaker K is closed. This proves that system topology change has little affect to our method.

D. Comparison With Existing Methods

In this subsection, we compare the proposed method with the existing arcing fault detection methods in the literature, including the high current arcing fault detection method proposed in [6] and the low current arcing fault detection method proposed in [12]. The data length is set be one cycle data and the sampling rate is 10 kHz. For this experiment, we pick 500 arcing faults including both high current and low current ones, and 500 non-arcing disturbances including all 3 types mentioned in Section IV.A. The results are shown in Table V. We can see that the proposed method has the highest detection accuracy for arcing fault and causes no false detection for non-arcing disturbances.

TABLE V
COMPARISON WITH EXISTING METHODS

Methods	Detection rate (%)	
	Arcing fault (500 cases in total)	Non-arcing disturbance (500 cases in total)
Method in [6]	92	85.2
Method in [12]	67	90
Proposed method	99.6	100

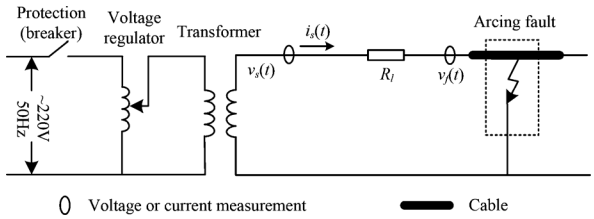

Fig. 12. The equivalent circuit of the arcing fault test system.

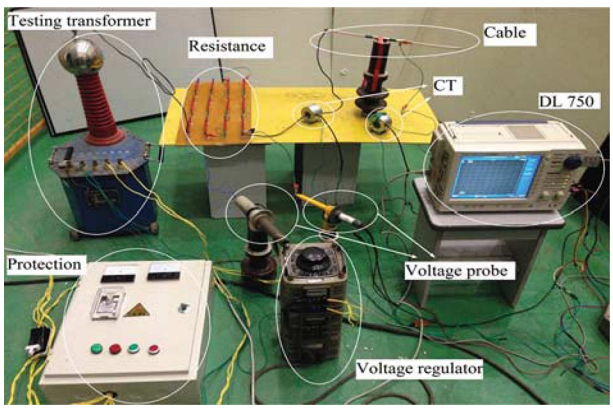

Fig. 13. The laboratory test of underground cable arcing fault.

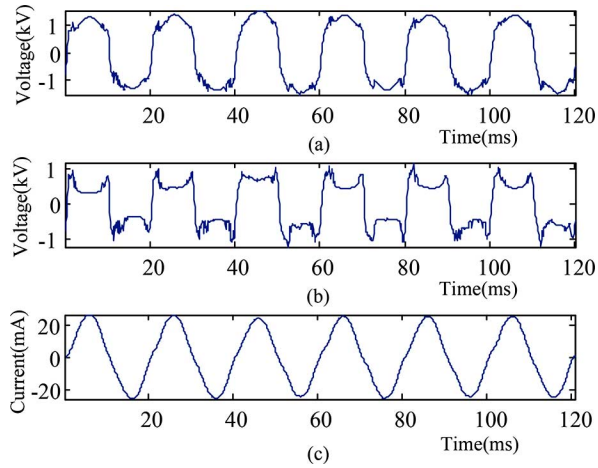

Fig. 14. Arcing fault waveforms in underground cable. (a) Voltage measured at substation $v_s(t)$. (b) Fault point voltage $v_f(t)$. (c) Feeder current $i_s(t)$ which is the same as the fault current.

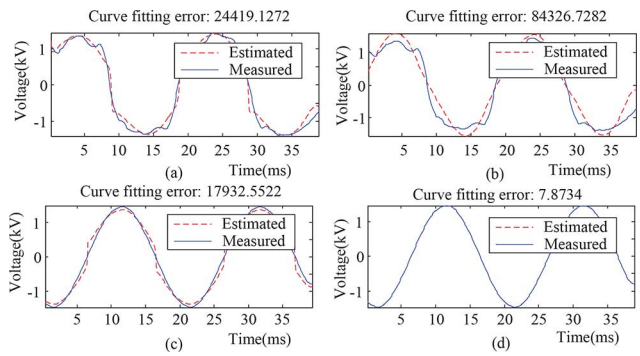

Fig. 15. Lab test results on bus voltage curve fitting. (a) Arcing fault voltage using the arc model. (b) Arcing fault voltage using the R-L model. (c) Constant impedance fault voltage using the arc model. (d) Constant impedance fault voltage using the R-L model.

The accuracy of the method in [12] is very low since it cannot detect high current arcing faults.

V. LABORATORY TEST RESULTS

To further validate the proposed method, experiments on underground cable arcing fault has been carried out in the laboratory. The equivalent circuit of the test is shown in Fig. 12, where $v_s(t)$ and $i_s(t)$ are the voltage and current at the sending end corresponding to the bus voltage and feeder current in a power system, R_l is the current limiting resistance corresponding to the transmission line resistance. $v_f(t)$ is the arc fault voltage when the cable is breakdown.

The laboratory test is as shown in Fig. 13. The main experiment setup consists of: 1) an AC 220 V (50 Hz) single-phase power source; 2) a voltage regulator (type: TSG2J-6); 3) a testing transformer (type: YDQ-10/100); 4) underground cable (type: YJV22-0.6/1 kV) and 5) waveform recorder (type: digital oscilloscope Yokogawa DL 750). In order to obtain frequent arcing faults, the cable was radially cut by a knife for a whole insulation layer. Then the knife was removed from cable insulation layer and the armour of the cable was restored.

The arcing breakdown in cable insulation is forced when v_f is larger than the cable insulation voltage by adjusting the voltage regulator. The bus voltage v_s, feeder current i_s and arc voltage v_f waveforms during arcing fault are shown in Fig. 14. It can be found that the voltage and current waveforms are similar to the simulation results shown in Figs. 7 and 8. The R_l is about 40 kohm. The cable is breakdown when v_s reaches 1.2 kV and the fault current is about 25 mA. The sampling rate is 10 kHz, i.e., 200 points/cycle for 50 Hz system. It is noted that the fault current is limited by the transformer capacity, so only low current arcing fault is generated in this experiment.

The proposed method is conducted on both arcing faults and non-arcing disturbances. The bus voltage curve-fitting comparison using the two assumed models (arcing fault model and R-L model) are shown in Fig. 15. For an arcing fault, as shown in Fig. 15(a) and (b), the curve-fitting error using the arc model is considerably smaller than that using the R-L model. It means that the proposed method can detect the arcing fault accurately. For a constant impedance fault, the R-L model based curve-fitting error is considerably smaller than that using the arcing fault model. So the proposed method does not cause false detection. We have conducted 3 arcing fault tests and 5 non-arcing disturbance tests, all arcing faults can be detected accurately and no false detection is raised by non-arcing disturbances. This validates the effectiveness of the proposed method.

VI. Conclusion

This paper proposes a new model-based detection scheme to discriminate arcing fault from other disturbances in MV distribution lines. We first derive accurate models to represent the behavior of substation voltage for both cases: an arcing fault occurs and a non-arcing disturbance occurs. The voltage drop on the distribution line is taken into consideration for the model accuracy. Then the detection problem is formulated into a binary hypothesis test. In solving the detection problem, least-squares parameter estimation and the minimum mean square-error detection rule are adopted.

The proposed scheme is general in the sense that it can detect both incipient fault in underground cable(high current arcing fault) and high impedance fault (low current arcing fault), it also can recognize transient fault in overhead line. The method is tested with several different types of arcing fault and non-arcing disturbances, different fault locations, different system structures, different noise level and a large number of disturbance events with different parameters. Simulation results show that the method has high accuracy and robustness when half-cycle or more data are used for detection. Lab experiments are also conducted, which validates that the proposed method is effective.

Acknowledgment

The authors gratefully acknowledge the direction of Prof. Kai Zhou, and the help of Min He, Jinwei Zuo and Jingyu He at Sichuan University for the laboratory tests on underground cable arcing fault.

References

[1] K. Abdolall *et al.*, "BC hydro 15 kV cable explosion.," *IEEE Trans. Power Del.*, vol. 17, no. 2, pp. 302–307, Apr. 2002.
[2] B. D. Russell and R. P. Chinchali, "A digital signal processing algorithm for detecting arcing faults on power distribution feeders.," *IEEE Trans. Power Del.*, vol. 4, no. 1, pp. 132–140, Jan. 1989.
[3] M. Sedighizadeh, A. Rezazadeh, and N. I. Elkalashy, "Approaches in high impedance fault detection a chronological review.," *Adv. Elect. Comput. Eng.*, vol. 10, no. 3, pp. 114–128, 2010.
[4] C. Benner, K. Butler-Purry, and B. Russell, Elect. Power Res. Inst., "Distribution fault anticipator," Palo Alto, CA, USA, Tech. Rep. 1001879, Dec. 2001.
[5] S. Kulkarni, S. Santoso, and T. A. Short, "Incipient fault location algorithm for underground cables.," *IEEE Trans. Smart Grid*, vol. 5, no. 3, pp. 1165–1174, May 2014.
[6] V. V. Terzija and Z. M. Radojevic, "Numerical algorithm for adaptive autoreclosure and protection of medium-voltage overhead lines.," *IEEE Trans. Power Del.*, vol. 19, no. 2, pp. 554–559, Apr. 2004.
[7] T. S. Sidhu and Z. Xu, "Detection of incipient faults in distribution underground cables.," *IEEE Trans. Power Del.*, vol. 25, no. 3, pp. 1363–1371, Jul. 2010.
[8] A. D. Stokes and W. T. Oppenlander, "Electric arcs in open air.," *J. Phys. D: Appl. Phys.*, vol. 21, no. 1, pp. 26–35, 1991.
[9] *IEEE Guide for Protective Relay Applications to Distribution Lines*, IEEE Standard C37.230-2007, Feb. 2008.
[10] Z. M. Radojevic and J. R. Shin, "New digital algorithm for adaptive reclosing based on the calculation of the faulted phase voltage total harmonic distortion factor.," *IEEE Trans. Power Del.*, vol. 22, no. 1, pp. 37–41, Jan. 2007.
[11] Z. M. Radojevic, V. Terzija, G. Preston, and S. Padmanabhan, "Smart overhead lines autoreclosure algorithm based on detailed fault analysis.," *IEEE Trans. Smart Grid*, vol. 4, no. 4, pp. 1829–1838, Dec. 2013.
[12] W. H. Kwon, G. W. Lee, Y. M. Park, and M. C. Yoon, "High impedance fault detection utilizing incremental variance of normalized even order harmonic power.," *IEEE Trans. Power Del.*, vol. 6, no. 2, pp. 557–564, Apr. 1991.
[13] A. Ghaderi, H. A. Mohammadpour, H. L. Ginn, and Y. J. Shin, "High-impedance fault detection in the distribution network using the time-frequency-based algorithm.," *IEEE Trans. Power Del.*, vol. 30, no. 3, pp. 1260–1268, Jun. 2015.
[14] I. Baqui, I. Zamora, J. Mazon, and G. Buigues, "High impedance fault detection methodology using wavelet transform and artificial neural networks.," *Elect. Power Syst. Res.*, vol. 81, no. 7, pp. 1325–1333, 2011.
[15] S. Gautam and M. Sukumar, "Detection of high impedance fault in power distribution systems using mathematical morphology.," *IEEE Trans. Power Syst.*, vol. 28, no. 2, pp. 1226–1234, May 2013.
[16] B. C. Levy, *Principles of Signal Detection and Parameter Estimation*. New York, USA: Springer, 2008.
[17] N. I. Elkalashy, M. Lehtonen, H. A. Darwish, M. A. Izzularab, and A.-K. I. Taalab, "Modeling and experimental verification of high impedance arcing fault in medium voltage networks.," *IEEE Trans. Dielect. Elect. Insul.*, vol. 14, no. 2, pp. 375–383, Apr. 2007.
[18] H. A. Darwish and N. I. Elkalashy, "Universal arc representation using EMTP.," *IEEE Trans. Power Del.*, vol. 20, no. 2, pt. 1, pp. 772–779, Apr. 2005.
[19] G. Parise, L. Martirano, and M. Laurini, "Simplified arc-fault model: The reduction factor of the arc current.," *IEEE Trans. Ind. Appl.*, vol. 49, no. 4, pp. 1703–1710, Jul. 2013.
[20] M. Kizilcay and T. Pniok, "Digital simulation of fault arcs in power systems.," *Eur. Trans. Elect. Power*, vol. 1, no. 1, pp. 55–60, Jan. 1991.
[21] G. I. Ospina, D. Cubillos, and L. Ibanez, "Analysis of arcing fault models," in *Proc. IEEE/Power Energy Soc. Transm. Distrib. Conf. Expo.: Latin Amer.*, 2008, pp. 1–5.
[22] M. Michalik, W. Rebizant, M. Lukowicz, and S. J. Lee, "High-impedance fault detection in distribution networks with use of wavelet-based algorithm.," *IEEE Trans. Power Del.*, vol. 21, no. 4, pp. 1793–1802, Oct. 2006.
[23] V. Torres, H. F. Ruiz, S. Maximov, and S. Ramirez, "Modeling of high impedance faults in electric distribution systems," in *Proc. IEEE Int. Autumn Meeting Power, Electron. Comput.*, 2014, pp. 1–6.
[24] S.-J. Lee *et al.*, "An intelligent and efficient fault location and diagnosis scheme for radial distribution systems.," *IEEE Trans. Power Del.*, vol. 19, no. 2, pp. 524–532, Apr. 2004.
[25] M. A. Redfern, S. C. Terry, and F. V. P. Robinson, "The application of distribution system current transformers for high frequency transient based protection," in *Proc. 8th Inst. Elect. Eng. Int. Conf. Develop. Power Syst. Protect.*, 2004, vol. 1, pp. 108–111.
[26] M. Kizilcay and K. H. Koch, "Numerical fault arc simulation based on power arc tests.," *Eur. Trans. Elect. Power*, vol. 4, no. 3, pp. 177–185, May 1994.
[27] B. Koch and P. Christophe, "Arc voltage for arcing faults on 25 (28)-kV cables and splices.," *IEEE Trans. Power Del.*, vol. 8, no. 3, pp. 779–788, Jul. 1993.
[28] A. Gaudreau and B. Koch, "Evaluation of LV and MV arc parameters.," *IEEE Trans. Power Del.*, vol. 23, no. 1, pp. 487–492, Jan. 2008.
[29] S. Kulkarni, A. J. Allen, S. Chopra, and S. Santoso, "Waveform characteristics of underground cable failures," in *Proc. IEEE Power Energy Soc. Gen. Meeting*, 2010, pp. 1–8.
[30] V. V. Terzija and H. J. Koglin, "On the modeling of long arc in still air and arc resistance calculation.," *IEEE Trans. Power Del.*, vol. 19, no. 3, pp. 1012–1017, Jul. 2004.
[31] J. C. Chen, B. T. Phung, D. M. Zhang, T. Blackburn, and E. Ambikairajah, "Study on high impedance fault arcing current characteristics," in *Proc. Australasian Univ., Power Eng. Conf.*, pp. 1–6.

Wenhai Zhang received the B.S. degree in electrical engineering from Sichuan University, Chengdu, China, in 2010, where he is currently pursuing the Ph.D. degree in electrical engineering.

From 2014 to 2015, he was a visiting Ph.D. student with the University of Alberta, Edmonton, AB, Canada. His research interests include single-line-to-ground fault detection and location in neutral uneffectively grounded system as well as arcing fault detection and location.

Yindi Jing (M'04) received the B.Eng. and M.Eng. degrees in automatic control from the University of Science and Technology of China, Hefei, China, in 1996 and 1999, respectively, and the M.Sc. and Ph.D. degrees in electrical engineering from California Institute of Technology, Pasadena, CA, USA, in 2000 and 2004, respectively.

From 2004 to 2005, she was a Postdoctoral Scholar in the Department of Electrical Engineering of the California Institute of Technology. From 2006 to 2008, she was a Postdoctoral Scholar in the Department of Electrical Engineering and Computer Science of the University of California, Irvine, CA, USA. In 2008, she joined the Electrical and Computer Engineering Department of the University of Alberta, Edmonton, AB, Canada, where she is currently an Associate Professor. She serves as an Associate Editor for the IEEE TRANSACTIONS ON WIRELESS COMMUNICATIONS and a member of the IEEE Signal Processing Society Signal Processing for Communications and Networking (SPCOM) Technical Committee. Her research interests are in massive multiple-input multiple-output systems, cooperative relay networks, training and channel estimation, robust detection, and fault detection in power systems.

Xianyong Xiao (M'13) received the B.S., M.S., and Ph.D. degrees in electrical engineering from Sichuan University, Chengdu, China, in 1990, 1998, and 2010, respectively.

Currently, he is a Professor in the College of Electrical Engineering and Information Technology at Sichuan University. His research interests are power quality, smart distribution systems, power system catastrophic events, uncertainty theory, and uncertainty measures applied to power systems.